Neutron skins and neutron stars

F. J. Fattoyev and J. Piekarewicz

Phys. Rev. C **86**, 015802 — Published 5 July 2012

DOI: 10.1103/PhysRevC.86.015802

Neutron skins and neutron stars

F. J. Fattoyev[1, 2, *] and J. Piekarewicz[1, †]

[1] *Department of Physics, Florida State University, Tallahassee, Florida 32306, USA*
[2] *Department of Physics and Astronomy, Texas A&M University-Commerce, Commerce, Texas 75429-3011, USA*

(Dated: June 5, 2012)

Background: The neutron skin of a heavy nucleus as well as many neutron-star properties are highly sensitive to the poorly constrained density dependence of the symmetry energy. **Purpose:** To provide for the first time meaningful theoretical errors and to assess the degree of correlation between the neutron-skin thickness of ^{208}Pb and several neutron-star properties. **Methods:** A proper covariance analysis based on the predictions of an accurately-calibrated relativistic functional *"FSUGold"* is used to quantify theoretical errors and correlation coefficients. **Results:** We find correlation coefficients of nearly one (or minus one) between the neutron-skin thickness of ^{208}Pb and a host of observables of relevance to the structure, dynamics, and composition of neutron stars. **Conclusions:** We suggest that a follow-up PREX measurement, ideally with a 0.5% accuracy, could significantly constrain the equation of state of neutron-star matter

PACS numbers: 21.65.Cd, 21.65.Mn, 26.60.Kp, 26.60.-c

I. INTRODUCTION

The equation of state (EOS) of neutron-rich matter plays a crucial role in understanding interesting phenomena in both nuclear physics and astrophysics, such as the limits of nuclear existence, the dynamics of heavy ion collisions, the structure of neutron stars, and the mechanism of core-collapse supernovae. A particularly important property of the EOS is the nuclear symmetry energy, whose value is well constrained by the ground-state properties of finite nuclei only near saturation density [1]. Given that the symmetry energy reflects the increase in the energy of the system as protons are turned into neutrons (or viceversa), many nuclear and astrophysical observables are sensitive to its density dependence. For example, the EOS of neutron-rich matter is the sole feature responsible for the structure of neutron stars. Moreover, the neutron-skin thickness of heavy nuclei—a system that is 18 orders of magnitude smaller than a neutron star—is also sensitive to the symmetry energy. This is because the slope of the symmetry energy is related to the pressure exerted by the neutrons in creating both a neutron-rich skin and the neutron-star radius [2, 3]. Although considerable effort has been devoted to the understanding of the EOS of isospin asymmetric matter and its possible impact on both laboratory and observational data [4, 5], our knowledge of the density dependence of the symmetry energy remains incomplete. Whereas some of the laboratory/observational data is relatively easy to collect, most requires great perseverance and ingenuity. Thus, in an effort to identify observables sensitive to the density dependence of the symmetry energy and to establish correlations among them, we rely on a powerful and systematic covariance analysis. Such a systematic statistical analysis may be used to attach meaningful uncertainty estimates to theoretical predictions [6]. Moreover, it can be used to identify observables that, although at present may be beyond experimental/observational reach, display a strong sensitivity to the symmetry energy. Finally, through such a covariance analysis one can quantify the degree of correlation between various observables. It is the aim of the present contribution to establish for the first time quantitative correlations between the neutron-skin thickness of ^{208}Pb and a variety of neutron-star observables.

In a recent publication we developed a covariance analysis within a class of relativistic mean-field models [7]. Starting from a χ^2-minimization procedure, we presented a step-by-step implementation of the statistical approach that provided quantitative uncertainties in our theoretical predictions as well as robust correlations among physical observables. In the present contribution we extend such a study to: (a) quantify the degree of correlation between the neutron-skin thickness of ^{208}Pb and several neutron-star properties and (b) provide meaningful theoretical uncertainties that arise from our incomplete knowledge of the density dependence of the symmetry energy. We have selected the neutron-skin thickness of ^{208}Pb as it represents a laboratory observable of paramount importance in constraining the density dependence of the symmetry energy. Indeed, the strong correlation between the neutron-skin thickness of ^{208}Pb and the slope of the symmetry energy at saturation density is a well established fact [1, 8–11]. Fur-

*Electronic address: Farrooh_Fattoyev@tamu-commerce.edu
†Electronic address: jpiekarewicz@fsu.edu

ther, the highly anticipated Lead Radius Experiment (PREX) has just provided the first model-independent evidence of the existence of a significant neutron skin in ^{208}Pb [12]. Building on the strength of the enormously successful parity-violating program at the Jefferson Laboratory, PREX used parity-violating electron scattering to determine the neutron-skin thickness of ^{208}Pb to be:

$$R_{\rm skin} \equiv R_n - R_p = 0.33^{+0.16}_{-0.18}\ {\rm fm}\ , \tag{1}$$

where $R_n(R_p)$ denotes the root-mean-square neutron(proton) radius. Although PREX achieved the systematic control required to perform this challenging experiment, unforeseen technical problems resulted in time losses that significantly compromised the statistical accuracy of the measurement. Thus, rather than achieving the original goal of a 1% error in the neutron radius, PREX had to settle for an error almost three times as large. Even so, the PREX measurement has already been used to impose some (mild) constraints on accurately-calibrated models of nuclear-structure [13]. Moreover, the—already approved—follow-up PREX measurement designed to achieve the original 1% goal will be of great value, especially if the unexpected large central value remains unchanged.

Since the strong correlation between the neutron-skin thickness of ^{208}Pb and the pressure of pure neutron matter near saturation density was first inferred [1, 8], a large number of additional correlations between $R_{\rm skin}$ and several neutron-star properties have been uncovered [4]. These include: (a) the crust-to-core transition density [3], (b) neutron-star radii [2, 14], (c) threshold density at the onset of the direct Urca process [15], and (d) the crustal moment of inertia [4, 16], among others. Although most of these correlations have been previously established through a systematic variation of a previously calibrated model, in the present manuscript we attempt for the first time to reliably quantify all these correlations via a legitimate covariance analysis. A covariance analysis represents the least biased and most exhaustive tool to uncover correlations between physical observables [7, 17].

The manuscript has been organized as follows. In Sec. II we briefly review the formalism required to implement the covariance analysis developed recently in Ref. [7]. In Sec. III we present physical arguments in favor of the expected correlations between the neutron-skin thickness of ^{208}Pb and several neutron-star properties. Properly estimated theoretical errors and correlation coefficients are also presented in this section. Finally, conclusions and suggestions for future work are summarized in Sec. IV.

II. FORMALISM

The covariance analysis mentioned above will be implemented using the predictions from the accurately calibrated FSUGold model [18]. The interacting Lagrangian density for the model—with its predictions generated at the relativistic mean-field (RMF) level—is given by

$$\begin{aligned}\mathscr{L}_{\rm int} &= \bar{\psi}\left[g_{\rm s}\phi - \Big(g_{\rm v}V_\mu + \frac{g_\rho}{2}\boldsymbol{\tau}\cdot\mathbf{b}_\mu + \frac{e}{2}(1+\tau_3)A_\mu\Big)\gamma^\mu\right]\psi \\ &- \frac{\kappa}{3!}(g_{\rm s}\phi)^3 - \frac{\lambda}{4!}(g_{\rm s}\phi)^4 + \frac{\zeta}{4!}g_{\rm v}^4(V_\mu V^\mu)^2 + \Lambda_{\rm v}g_\rho^2\,\mathbf{b}_\mu\cdot\mathbf{b}^\mu g_{\rm v}^2 V_\nu V^\nu\ .\end{aligned} \tag{2}$$

This model contains an isodoublet nucleon field (ψ) interacting via the exchange of two isoscalar mesons, the scalar sigma (ϕ) and the vector omega (V^μ), one isovector meson, the rho ($\mathbf{b}^\mu$), and the photon (A^μ). In order to improve the standing of the model the Lagrangian density is supplemented by scalar and vector self-interactions. In particular, the scalar self-interaction (with coupling constants κ and λ) is responsible for reducing the compression modulus of nuclear matter from the unrealistically large value of $K=545$ MeV obtained with the original Walecka model [19, 20] to about $K=230$ MeV. Such a significantly lower value for the compression modulus is demanded by measurements of giant monopole resonances in medium to heavy nuclei [21–24]. The quartic isoscalar-vector self-interaction is responsible for softening the EOS at high densities. Indeed, by tuning ζ one can generate different limiting neutron-star masses without modifying the behavior of the EOS around saturation density [25]. As such, ζ is fairly insensitive to laboratory observables and must be constrained from astrophysical observations. Finally, the mixed quartic vector interaction (as described by parameter $\Lambda_{\rm v}$) was introduced to modify the density dependence of symmetry energy [2], which is fairly stiff in the original Walecka model. By calibrating the parameters of the model using both ground-state properties of finite nuclei as well as their collective excitations [18], the FSUGold model has been fairly successful when compared against theoretical, experimental, and observational constraints [26]. However, as more observational and experimental data become available—such as the recently reported 2-solar mass neutron star [27]—further refinements may be required [28] (for example by tuning ζ). Yet, for the purpose of this contribution we will be satisfied with the use of the FSUGold model as the basis for the covariance analysis. We note that whereas the IU-FSU parametrization has been adjusted to account for the existence of a 2-solar mass neutron star [28], such an adjustment was not based on the minimization of a suitably-defined quality function. Thus, a proper covariance analysis is not possible for the

IU-FSU case. However, given that the IU-FSU parametrization was obtained through a fine tuning of the accurately-calibrated FSUGold interaction, we expect the emergence of similar correlations in both models. An updated density functional based on the minimization of a quality function that incorporates new observational data is presently under construction.

The covariance analysis follows closely the approach outlined in Refs. [7, 17] which, in turn, is based on the comprehensive text by Brandt [29]. The derivation, implementation, and power of the formalism was illustrated in our recent study using two relativistic mean-field models [7]. Thus, in the present contribution we only offer a brief summary. The covariance analysis starts with the definition of the quality measure χ^2. That is,

$$\chi^2(\mathbf{p}) \equiv \sum_{n=1}^{N} \left(\frac{\mathcal{O}_n^{(\mathrm{th})}(\mathbf{p}) - \mathcal{O}_n^{(\mathrm{exp})}}{\Delta\mathcal{O}_n} \right)^2 , \tag{3}$$

where N denotes the total number of selected observables that will be employed in the calibration procedure. Each of the observables, $\mathcal{O}_n^{(\mathrm{exp})}$, is assumed to have been determined experimentally with an accuracy of $\Delta\mathcal{O}_n$, which acts as a weight factor in the quality measure. In addition, each of the N observable is computed within the model $\mathcal{O}_n^{(\mathrm{th})}(\mathbf{p})$ as a function of the F model-parameters $\mathbf{p}=(p_1,\ldots,p_F)$. The calibration procedure terminates when a set of optimal parameters $\mathbf{p}_0$ are found that minimize the quality measure.

Given that our main goal is not the minimization procedure, but rather the estimation of theoretical uncertainties and the assessment of correlations among observables, we use a set of nuclear properties generated directly from the FSUGold model. This guarantees that the quality measure so defined is minimized. In particular, the following set of $N=8$ observables have been selected as input for χ^2: (1) the saturation density ρ_0, (2) the binding energy per particle of symmetric nuclear matter at saturation density ε_0, (3) the binding energy per particle of symmetric nuclear matter at twice saturation density $\varepsilon(2\rho_0)$, (4) the compression modulus of symmetric nuclear matter K_0, (5) the effective (Dirac) mass of symmetric nuclear matter at saturation density $M_0^\star$, (6) the symmetry energy $\tilde{J}$ evaluated at a sub-saturation density of $\rho\approx 0.1\,\mathrm{fm}^{-3}$, (7) the slope of the symmetry energy at saturation density L, and (8) the maximum neutron-star mass $M_{\max}$. We attach a 2% uncertainty to all of the observables—except for the case of the slope of the symmetry energy L where the significantly larger value of 20% is assumed. Such a large uncertainty reflects our poor understanding of the density dependence of the symmetry energy. Note that our choice of $\tilde{J}$, namely, the symmetry energy at sub-saturation density rather than at saturation density, follows from the fact that heavy nuclei constrain the symmetry energy at a density which is intermediate between the center and the surface of the nucleus. Indeed, at such a sub-saturation density the theoretical uncertainties appear to be minimized [1].

Having obtained the optimal parameter set $\mathbf{p}_0$ through the minimization of the quality measure, one can the proceed to compute and diagonalize the symmetric matrix of second derivatives. This matrix contains all the information about the behavior of the χ^2 function around the minimum. That is,

$$\chi^2(\mathbf{p}) - \chi^2(\mathbf{p}_0) \equiv \Delta\chi^2(\mathbf{x}) = \mathbf{x}^T \hat{\mathcal{M}}\, \mathbf{x} = \boldsymbol{\xi}^T \hat{\mathcal{D}} \boldsymbol{\xi} = \sum_{i=1}^{F} \lambda_i \xi_i^2 , \tag{4}$$

where

$$x_i \equiv \frac{(\mathbf{p}-\mathbf{p}_0)_i}{(\mathbf{p}_0)_i} \tag{5}$$

are scaled dimensionless variables, $\hat{\mathcal{M}} = \hat{\mathcal{A}}\hat{\mathcal{D}}\hat{\mathcal{A}}^T$, and $\boldsymbol{\xi} = \hat{\mathcal{A}}^T\mathbf{x}$ are dimensionless variables in a rotated basis. Here $\hat{\mathcal{A}}$ is the orthogonal matrix whose columns are composed of the normalized eigenvectors and $\hat{\mathcal{D}} = \mathrm{diag}(\lambda_1,\ldots,\lambda_F)$ is the *diagonal* matrix of eigenvalues. Although the full covariance analysis may be carried out without the need to diagonalize the matrix of second derivatives $\hat{\mathcal{M}}$, doing so is both simple and illuminating. For example, the small oscillations around the χ^2-minimum may be represented as a collection of F uncoupled harmonic oscillators. Doing so readily identifies the *"stiff"* and *"soft"* modes in parameter space. In particular, the soft modes indicate the linear combination of parameters that are poorly constrained by the choice of observables included in the quality measure. In turn, this suggets the kind of additional physical observables that are required to further constrain the model. In the particular case of FSUGold, the softest direction is dominated by the *"in-phase motion"* of the isovector coupling constants g_ρ and Λ_{v} [7]. This particular linear combination remains largely unconstrained because of our poor knowledge of the density dependence of the symmetry energy.

To obtain meaningful theoretical uncertainties as well as to assess the degree of correlation between two observables, one must compute the statistical covariance of two observables A and B. Assuming that the model parameters are

distributed according to quality measure as $\exp\left(-\mathbf{x}^T\hat{\mathcal{M}}\,\mathbf{x}/2\right)$, the covariance of A and B may be written as follows:

$$\mathrm{cov}(A,B) = \sum_{i,j=1}^{F} \frac{\partial A}{\partial x_i}(\hat{\mathcal{M}}^{-1})_{ij}\frac{\partial B}{\partial x_j} = \sum_{i=1}^{F} \frac{\partial A}{\partial \xi_i}\lambda_i^{-1}\frac{\partial B}{\partial \xi_i}\ . \tag{6}$$

Note that the variance $\sigma^2(A)$ of a given observable A is simply given by $\sigma^2(A) = \mathrm{cov}(A,A)$. Also note that, all other things being equal, the $\mathrm{cov}(A,B)$ is dominated by the softest direction. Finally, the Pearson product-moment correlation coefficient—or correlation coefficient for simplicity—is defined as:

$$\rho(A,B) = \frac{\mathrm{cov}(A,B)}{\sqrt{\mathrm{var}(A)\mathrm{var}(B)}}\ . \tag{7}$$

Further details on the covariance analysis may be found in Refs. [7, 17, 29].

III. RESULTS

The main goal of this contribution is to use a covariance analysis to reliably assess the correlation between the neutron-skin thickness of ^{208}Pb ($R_{\rm skin}$) and a large number of observables of relevance to the structure, dynamics, and composition of neutron stars. Moreover, we rely on a covariance analysis to attach meaningful uncertainty estimates to our theoretical predictions. In particular, the FSUGold model predicts the following neutron-skin thickness of ^{208}Pb with properly computed theoretical errors [7]:

$$R_{\rm skin} = (0.2069 \pm 0.0366)\,\mathrm{fm}\ [17.698\%]\ . \tag{8}$$

Note that this prediction fits comfortably within the recently determined value by the PREX collaboration [see Eq. (1)]. However, there is a significant difference in the central value that may prove very interesting if the follow-up PREX measurement can significantly reduce the error bars without dramatically affecting the central value.

Given the large number of observables that will be discussed, the present section has been divided into several subsections. In particular, each subsection motivates the connection of a given neutron-star observable to $R_{\rm skin}$ and discusses its relevance in constraining the density dependence of the symmetry energy in regions that may be inaccessible to laboratory experiments.

A. Pure Neutron Matter

Assuming the validity of General Relativity, the equation of state of cold, catalyzed neutron-rich matter is the sole ingredient that determines the structure of spherical neutron stars in hydrostatic equilibrium. As such, one of the most stringent constraints on the structure of neutron stars comes from the EOS of pure neutron matter (PNM). Although PNM remains a theoretical construct, enormous progress has been made in constraining its equation of state at low densities. Interestingly enough, most of the progress in this area has been driven by remarkable advances in cold-atom experiments that make possible to study the universal behavior of resonant Fermi gases at the unitary limit of infinite scattering length. Even though the appreciable effective range of the neutron-neutron interaction invalidates some of the powerful arguments associated with resonant Fermi gases, model independent results have been obtained for dilute neutron matter [30]. Moreover, the full power of quantum Monte Carlo methods has been used to extend the calculations to higher densities [31–33]. By doing so, the calculated EOS—which matches smoothly to the analytic results—provides important constraints on nuclear density functionals. Indeed, the impact of such constraints can be clearly assessed in Fig. 1 where the equation of state of pure neutron matter for a variety of microscopic approaches (see Refs. [31, 32] and references therein) is displayed alongside the predictions from three relativistic functionals. Note that although not included in the calibration procedure, the EOS predicted by the FSUGold interaction (solid blue line) appears consistent with most of the microscopic approaches. Also note that the required *"softening"* of the EOS relative to the more traditional RMF models (such as NL3) was generated by constraining the calibration procedure by the dynamics of nuclear collective modes [18].

The wide (blue) band in Fig. 1 represents the 1σ uncertainty in the predictions of the FSUGold model. That the 1σ-band is so wide reflects our poor understanding of the density dependence of the symmetry energy (recall that a 20% uncertainty was assumed for the slope of the symmetry energy L). In order to reduce such a large uncertainty one must constrain L—or equivalently the pressure of PNM at saturation—through an accurate measurement of the neutron radius in ^{208}Pb. Although the correlation between the neutron radius of ^{208}Pb and the slope of the symmetry

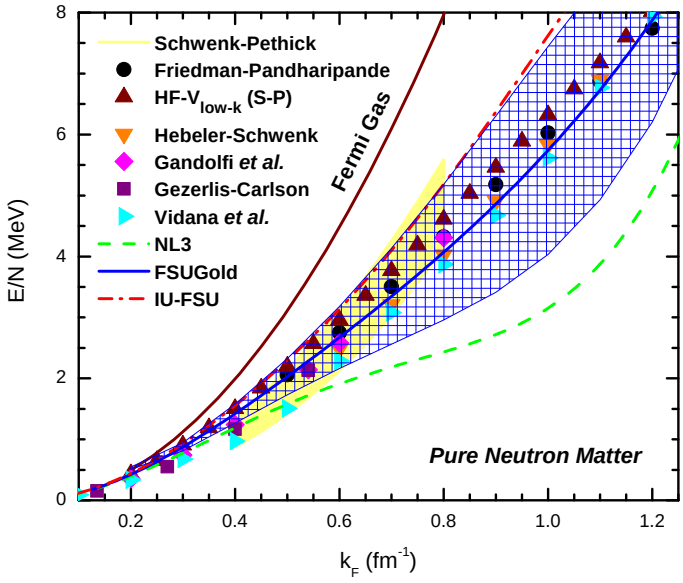

FIG. 1: (Color online) Theoretical uncertainties in the energy per neutron as a function of the Fermi momentum for pure neutron matter. The shaded blue area are the 1σ theoretical uncertainty associated to the FSUGold model.

energy L is by now very well established, only recently has a statistically meaningful correlation coefficient between such quantities been computed [7, 17]. We have now extended such a covariance analysis to explore the correlation between the neutron-skin thickness of ^{208}Pb and the pressure of PNM at half, one, and two times nuclear-matter saturation density (see Table I and Fig. 2).

A	$\langle A\rangle \pm \Delta A$	$\rho(A, R_{\rm skin})$
L(MeV)	(60.5152 ± 12.1011) [19.997%]	0.9952
$P(\rho_0)$	(3.1842 ± 0.6349) [19.940%]	0.9882
$P(\rho_0/2)$	(0.4874 ± 0.1721) [35.304%]	0.9861
$P(2\rho_0)$	(21.8569 ± 1.2735) [5.827%]	0.8016

TABLE I: Theoretical errors associated to the predictions of the FSUGold model for the slope of the symmetry energy and the pressure of pure neutron matter (in units of MeV fm^{-3}) at three different densities.

Given that the symmetry energy is to a very good approximation equal to the difference in energy between PNM and symmetric nuclear matter, the slope of the symmetry energy L is closely related to the pressure of PNM at saturation density, *i.e.*, $P(\rho_0) \approx \rho_0 L/3$. Thus, perhaps not surprisingly, we find correlation coefficients of almost one between $R_{\rm skin}$ and both L and $P(\rho_0)$. Note, however, that the correlation remains as strong for the pressure of PNM at half saturation density $P(\rho_0/2)$—but deteriorates significantly for the pressure at twice saturation density $P(2\rho_0)$. This last fact reflects the insensitivity of finite-nuclei observables to the high-density component of the equation of state.

B. Neutron-Star Radii

The structure of neutron stars—particularly the mass-radius relation—depends critically on the equation of state of neutron-rich matter. In particular, neutron-star radii provide stringent constraints on the density dependence of the symmetry energy. Ideally, one would measure neutron-star radii over a broad range of masses. Indeed, measuring neutron-star radii $R(M)$ for a large range of neutron star masses M would allow one to directly deduce the EOS [34]. Unfortunately, whereas various neutron-star masses are accurately known [35], a precise determination of their radii does not yet exist. Moreover, constraining the EOS at low densities from the radii of low-mass neutron stars may be

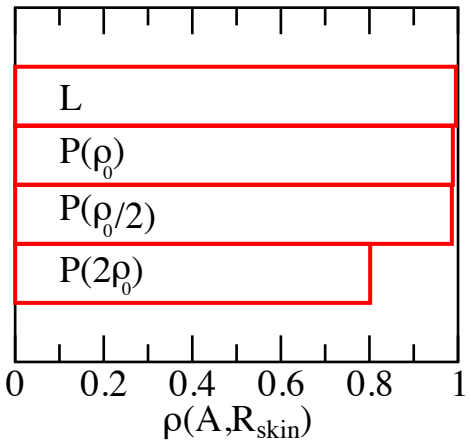

FIG. 2: (Color online) The correlation coefficient between the neutron-skin thickness of ^{208}Pb and the slope of the symmetry energy L and the pressure of pure neutron matter at three values of the density.

difficult as these may be very rare. However, the low-density EOS may be constrained from the neutron radii of heavy nuclei as these contain similar information [2, 14]. This is because the same pressure that is responsible for supporting a (low-mass) neutron-star against gravitational collapse is also responsible for the development of a neutron-rich skin in heavy nuclei. Indeed, theoretical predictions suggest a strong correlation between these two observables: *the larger the neutron skin of a heavy nucleus, the larger the stellar radius.*

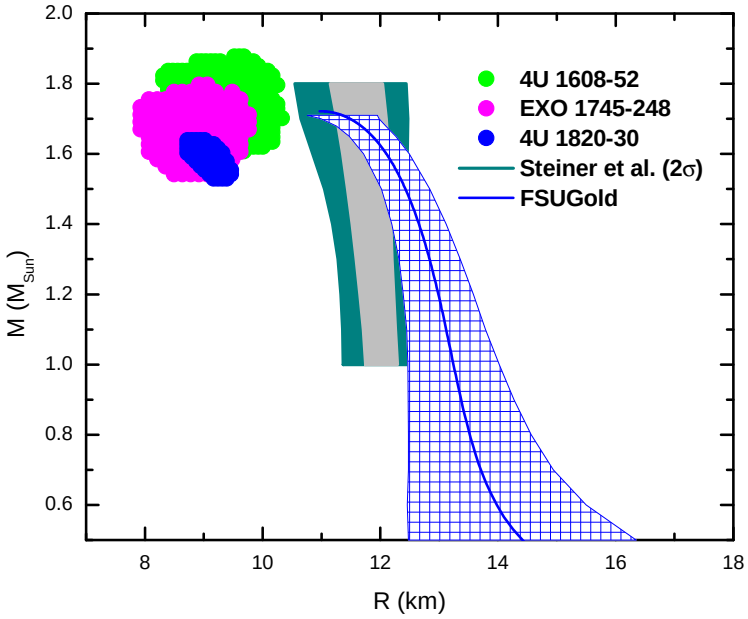

FIG. 3: (Color online) Theoretical predictions for the mass-versus-radius relation of neutron stars calculated within 1σ uncertainty in the FSUGold model. The observational data that suggest very small stellar radii represent 1σ confidence contours for the three neutron stars reported in Ref. [36]. The two shaded areas that suggest larger radii are 1σ and 2σ contours extracted from the analysis of Ref. [37].

To quantify the theoretical uncertainties in neutron-star radii and to assess their correlation to $R_{\rm skin}$, we display in Fig. 3 the *Mass-vs-Radius* relation predicted by the FSUGold model. Although the determination of neutron-star radii from observations of the luminosity and temperature is both challenging and hindered by uncertainties in models

of the stellar atmosphere (see Ref. [38] and references therein) significant advances in X-ray astronomy have allowed the simultaneous determination of masses and radii from a systematic study of several X-ray bursters [36, 37]. Results from such studies are displayed in Fig. 3 alongside the FSUGold predictions. We should note that while we believe that studies of X-ray bursters will eventually become instrumental in constraining the dense matter equation of state, at present they suffer from systematic uncertainties [37]. For example, the analysis from Ref. [36] (occupying the upper left-hand corner of the figure) suggests very small radii that are difficult to reconcile with the predictions from relativistic mean-field models [39]. In contrast, the more recent analysis by Steiner, Lattimer, and Brown [37] suggests significantly larger neutron-star radii that appear consistent with the predictions of the model. However, even the more conservative analysis of Ref. [37] has been recently called into question [40]. Indeed, the authors of Ref. [40] propose a lower limit on the stellar radius of 14 km for masses below $2.3\,\mathrm{M}_\odot$, thereby suggesting a fairly stiff equation of state. Note that the wide (blue) band in Fig. 3 denotes our theoretical uncertainties in the predictions of the stellar radii. We observe that whereas the stellar radius is fairly well constrained for large-mass neutron stars, radii of low-mass stars display large theoretical errors. For example, the radius of a $M = 1.4 M_\odot$ neutron star is determined with a 3.6% uncertainty (Table II). Yet the error grows by a factor of three for a $M = 0.6 M_\odot$ neutron star. Such behavior is dominated by the large uncertainty in L. Whereas the radius of a heavy neutron star is sensitive to the equation of state at both intermediate and high densities, the radii of low-mass neutron stars is sensitive to the range of densities probed in heavy nuclei. Indeed, FSUGold predicts a central density in a $M = 0.5 M_\odot$ neutron star of 0.21 fm^{-3}, only slightly higher than saturation density. Due to the large sensitivity of neutron stars radii to L, a correlation between the neutron-skin thickness of ^{208}Pb and stellar radii has been established [2, 3, 14]. Moreover, we expect a stronger correlation between $R_{\rm skin}$ and the radii of low-mass neutron stars than between $R_{\rm skin}$ and the radii of massive stars. This fact is clearly borne out by the results displayed in Table II and Fig. 4.

A	$\langle A\rangle \pm \Delta A$	$\rho(A, R_{\rm skin})$
$R_{0.6}$	(13.9785 ± 1.5183) [10.862%]	0.9953
$R_{0.8}$	(13.5204 ± 1.0446) [7.726%]	0.9931
$R_{1.0}$	(13.2439 ± 0.7776) [5.872%]	0.9866
$R_{1.2}$	(12.9864 ± 0.5964) [4.593%]	0.9770
$R_{1.4}$	(12.6568 ± 0.4603) [3.637%]	0.9486
$R_{1.6}$	(12.1038 ± 0.3881) [3.206%]	0.8361

TABLE II: Theoretical errors associated to the predictions of the FSUGold model for the radii (in km) of neutron stars of various masses. Note that the subscript indicates the neutron-star mass in solar masses.

C. Direct Urca Process

Neutron stars are born very hot (with a temperature of about 10^{11} K) and cool rapidly via neutrino emission through the direct *"Urca" process* involving neutron beta decay and electron capture [41–44]:

$$n \to p + e^- + \bar{\nu}_e \,, \tag{9a}$$

$$e^- + p \to n + \nu_e \,. \tag{9b}$$

After most of the *"neutronization"* process is complete, the standard cooling scenario assumes that neutrino emission proceeds through the *modified Urca* process:

$$n + n \to n + p + e^- + \bar{\nu}_e \,. \tag{10}$$

However, given that the modified Urca process requires the presence of a bystander nucleon to conserve momentum, this process may be millions of times slower relative to the direct Urca rate [43]. The putative transition into the significantly slower modified Urca phase is solely based on the assumption that the proton fraction in the stellar core is below the $\sim$15% required to conserve momentum at the Fermi surface. However, such an assumption is suspect as the proton fraction is determined entirely by the density dependence of the symmetry energy, which remains poorly constrained. In particular, a stiff symmetry energy, namely, one that increases rapidly with density, favors large proton fractions and this may facilitate some enhanced cooling. Note, however, that unlike other enhanced-cooling scenarios that may involve the presence of exotic particles in the core, this enhanced-mechanism is not exotic as it only involves standard particles and a relatively stiff nuclear symmetry energy. Also note that recent X-ray observations by the Chandra observatory seem to suggest that some neutron stars may indeed require some form of enhanced cooling (see [44] and references therein).

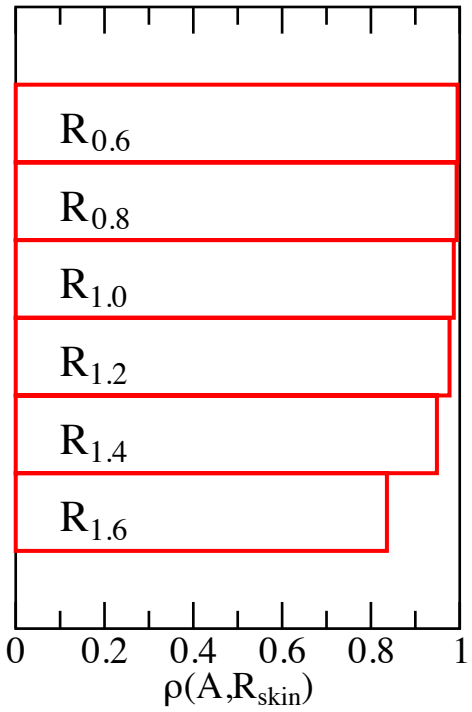

FIG. 4: (Color online) The correlation coefficient between the neutron-skin thickness of ^{208}Pb and the radius of neutron stars of a variety masses. Note that the subscript indicates the neutron-star mass in solar masses.

Given that the proton fraction in neutron-star matter is controlled by the density dependence of the symmetry energy, a strong correlation between the onset of the direct Urca process and the neutron-skin thickness of ^{208}Pb has been established [15]. Momentum conservation at the Fermi surface demands that the sum of the Fermi momenta of the protons and electrons must be greater than or equal than the neutron Fermi momentum. That is,

$$k_{\rm F}^{\rm n} \leq k_{\rm F}^{\rm p} + k_{\rm F}^{\rm e} \; . \tag{11}$$

The onset for the direct Urca process ($k_{\rm F}^{\rm n} \equiv k_{\rm F}^{\rm p} + k_{\rm F}^{\rm e}$) together with the condition of charge neutrality is sufficient to determine the threshold proton fraction:

$$Y_{\rm p}^{\rm Urca} = \left[1 + (1 + x_{\rm e}^{1/3})^3\right]^{-1} \underset{x_{\rm e}=1}{\longrightarrow} \frac{1}{9} \approx 0.11 \; . \tag{12}$$

In the above expression $x_{\rm e}$ is the electron-to-proton fraction and the arrow indicates the model-independent limit of 1/9 for the case of a vanishing muon fraction ($x_\mu = 1 - x_{\rm e} = 0$). For the realistic case of a non-zero muon fraction, the threshold proton fraction is model dependent and increases slightly to about $Y_{\rm p}^{\rm Urca} \lesssim 0.15$. In particular, FSUGold predicts a threshold proton fraction of $Y_{\rm p}^{\rm Urca} = 0.137$. That is, the FSUGold model predicts that if the proton fraction within the neutron star exceeds this threshold value, then enhanced cooling via the direct Urca process is possible. Note that this threshold proton fraction is reached at a density of about three times saturation density which corresponds to the central density of a $M_{\rm Urca} = 1.30\, M_\odot$ neutron star (see Table III). This suggests—in the particular case of the FSUGold model—that any neutron star with a mass below $1.30\, M_\odot$ that displays enhanced cooling is likely to contain an exotic core. For comparison, we should mention that for the significantly stiffer NL3 equation of state, the threshold proton fraction ($Y_{\rm p}^{\rm Urca} = 0.129$) is reached at the significantly lower density of $\rho_{\rm Urca} = 0.205$ fm^{-3}. This would imply that any neutron star with a mass in excess of $0.84\, M_\odot$ will cool rapidly by the direct Urca process. Finally, we note that regardless of the model, the muon-to-proton fraction at the threshold density is fairly significant; of the order of 30-40%.

To quantify the strong correlation between various neutron-star properties at the Urca threshold and the neutron-skin thickness of ^{208}Pb, we have listed in Table III and plotted in Fig. 5 the corresponding theoretical errors and correlation coefficients extracted from our covariance analysis. As suggested above, we find a strong direct correlation between the proton fraction at high densities and $R_{\rm skin}$. Note, however, that at low densities the proton fraction and $R_{\rm skin}$ become *anti*-correlated, as a stiff symmetry energy goes to zero faster than a soft one. Moreover, as expected, the

A	$\langle A\rangle \pm \Delta A$	$\rho(A, R_{\rm skin})$
$\rho_{\rm Urca}$	(0.4668 ± 0.1324) [28.359%]	-0.9928
$M_{\rm Urca}/M_\odot$	(1.3012 ± 0.2658) [20.427%]	-0.9927
$Y_{\rm p}^{\rm Urca}$	(0.1367 ± 0.0019) [1.421%]	-0.9927
$Y_{\rm p}(2\rho_0)$	(0.1064 ± 0.0138) [13.000%]	$+0.9906$
$Y_{\rm p}(\rho_0)$	(0.0609 ± 0.0055) [9.055%]	$+0.9166$
$Y_{\rm p}(\rho_0/2)$	(0.0346 ± 0.0051) [14.651%]	-0.9063

TABLE III: Theoretical errors associated to the predictions of the FSUGold model for various neutron-star properties of relevance to the direct Urca process. The threshold density is given in units of fm^{-3}.

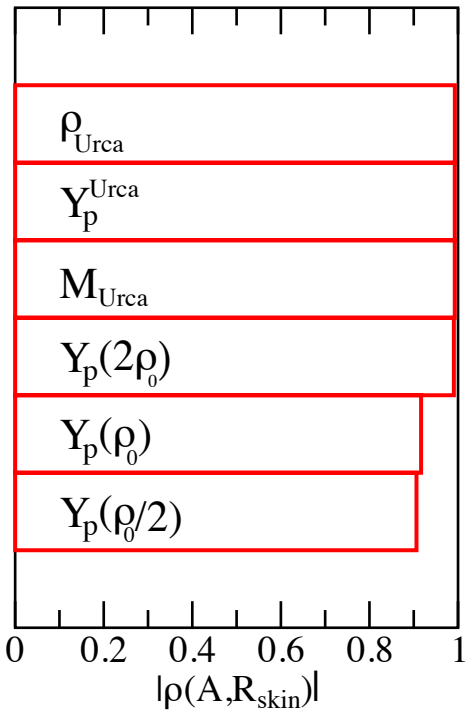

FIG. 5: (Color online) The correlation coefficient between the neutron-skin thickness of ^{208}Pb and various neutron-star properties of relevance to the direct Urca process.

Urca threshold density, stellar mass, and proton fraction display a strong (inverse) correlation to $R_{\rm skin}$. In particular, we note that the strong anti-correlation between $Y_{\rm p}^{\rm Urca}$ and $R_{\rm skin}$ emerges entirely because of the presence of muons in the star. Indeed, without muons $Y_{\rm p}^{\rm Urca}$ is fixed at 1/9 so all of its derivatives with respect to the model parameters will vanish and, thus, so will the correlation coefficient [see Eq. (6)]. Finally, we have shown that a thin neutron skin in ^{208}Pb, *i.e.,* a very soft symmetry energy, requires a large neutron-star mass for the onset of the direct Urca process. Thus, we believe that the observation of enhanced cooling in low-mass neutron stars ($M < M_{\rm Urca}$) provides one of the most promising indicators of exotic states of matter residing in the stellar cores. Note that our model is a *"minimal"* one in the sense that no exotic constituents are considered. We adhere to this minimal scenario because the interactions of exotic particles—such as hyperons—is poorly known, especially at the extreme densities found in the stellar cores. What is fairly uncontroversial, however, is that the onset of strangeness is likely to be accompanied by a softening of the equation of state. Such a softening is characterized by higher central densities (for a given stellar mass), a lower limiting mass, and smaller stellar radii. The impact of such a strangeness-induced softening on various stellar properties, such as its maximum mass, stellar radii, proton fraction, and Urca threshold, has been recently addressed in Refs. [45, 46] (and references therein).

D. Core-Crust Transition

Neutron stars have a solid crust above a uniform liquid core. The structure and composition of the solid crust remains a source of significant debate and of considerable interest [47–58]. Moreover, the crust is believed to be of critical importance in a variety of fascinating astrophysical phenomena, such as pulsar glitches, giant magnetar flares, and the emission of gravitational waves [59–62]. The phase transition from the solid crust to the uniform liquid core depends on the properties of neutron-rich matter. As neutron-rich matter becomes dilute, the uniform ground state becomes unstable against small-amplitude density fluctuations [3, 14]. That is, it becomes energetically favorable for the system to fragment into high-density clusters (*i.e.,* nuclei) embedded in a dilute neutron-rich vapor. Yet details of the transition depend sensitively on the proton fraction—and thus on the density dependence of the symmetry energy—at low densities. Whereas the proton fraction at high density displays a direct correlation to the neutron-skin thickness of ^{208}Pb, the proton fraction at low densities is *anti-correlated* to $R_{\rm skin}$. For example, the correlation coefficient between $Y_{\rm p}(\rho_0/2)$ and $R_{\rm skin}$ is both large and *negative* (see Table III). Given that the symmetry energy represents the energy cost in departing from the isospin symmetric limit, a stiff symmetry energy falls rapidly to zero at low densities and, hence, tolerates a larger isospin asymmetry (*i.e.,* smaller $Y_{\rm p}$) than their softer counterparts. Thus, a lower proton fraction typically implies a low transition density from the solid crust to the liquid core. This suggests an inverse correlation: *the thicker the neutron skin thickness of ^{208}Pb, the lower the core-crust transition density* [3].

A	$\langle A\rangle \pm \Delta A$	$\rho(A, R_{\rm skin})$
$P_{\rm t}$	(0.4020 ± 0.1071) [26.640%]	+0.9474
$Y_{\rm p}^{\rm t}$	(0.0351 ± 0.0069) [19.711%]	−0.9260
$\mathcal{E}_{\rm t}$	(71.5337 ± 5.3747) [7.514%]	−0.9207
$\rho_{\rm t}$	(0.0755 ± 0.0056) [7.369%]	−0.9203

TABLE IV: Theoretical errors associated to the predictions of the FSUGold model for various neutron-star properties of relevance to the transition between the solid crust and the uniform liquid core. The transition pressure and energy density are given in units of MeV fm^{-3} and the transition baryon density in fm^{-3}.

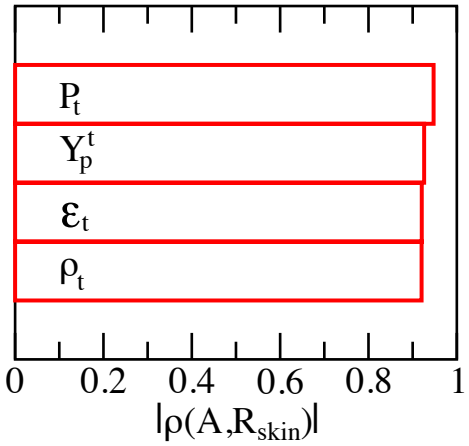

FIG. 6: (Color online) The correlation coefficient between the neutron-skin thickness of ^{208}Pb and various neutron-star properties of relevance to the transition between the solid crust and the uniform liquid core.

Several approaches—of both a microscopic and thermodynamic nature—have been used to determine the instability of the uniform ground-state against cluster formation [3, 14, 58, 63–65]. In the present study we rely on the RPA stability analysis described in Ref. [14] to compute the baryon density, proton fraction, pressure, and energy density at the core-crust interface. Results from the covariance analysis are listed in Table IV and displayed in Fig. 6. For comparison, the stiffer NL3 equation of state—which has a significantly smaller symmetry energy at sub-saturation densities than FSUGold—predicts the following significantly lower values: $\rho_t = 0.052\,{\rm fm}^{-3}$, $Y_p^{\rm t} = 0.015$, $P_t = 0.212\,{\rm MeV\,fm}^{-3}$, and $\mathcal{E}_t = 48.960\,{\rm MeV\,fm}^{-3}$. As suggested earlier, models with a stiffer symmetry energy and thus thicker neutron skins, display a *"delayed"* transition from the uniform core to the solid crust. Thus, we find a strong anti-correlation between $R_{\rm skin}$ and the various stellar properties at the core-crust interface [3]. Yet, the transition pressure $P_{\rm t}$ behaves in an interesting and unique way. First, in contrast to other observables, $P_{\rm t}$ appears to be

directly correlated to $R_{\rm skin}$ with a large and positive correlation coefficient of about 0.95. Second, the mere existence of a strong correlation appears to be at odds with earlier studies that suggest a weak correlation between $P_{\rm t}$ and $R_{\rm skin}$ [16, 63, 65]. We attribute the present intriguing result to the fact that within the realm of a covariance analysis, the correlation coefficient between two observables is obtained by generating model parameters that are distributed according to the quality measure [see Eq. (4)]. That is, models that differ significantly from the optimal (FSUGold) model carry little weight. In contrast, the weak correlation between $P_{\rm t}$ and $R_{\rm skin}$ suggested in Ref. [16] was obtained through a systematic (perhaps even *ad-hoc*) variation around the optimal model. Although the covariance analysis implemented here provides the proper statistical measure of correlation between two observables [29], a covariance analysis can not assess *systematic* errors associated with the limitations of a given model. Thus, whereas the FSUGold model—with its soft symmetry energy—predicts a strong positive correlation between $P_{\rm t}$ and $R_{\rm skin}$, a model with a stiffer EOS may predict exactly the opposite (see Fig. 6 of Ref. [16]).

E. Stellar Moment of Inertia

Although the general-relativistic expression for the moment of inertia of a neutron star is fairly complex—even in the so-called *slow-rotation approximation* [66, 67]—on simple dimensional grounds it must scale as the product of the stellar mass times the *square* of its radius. Thus, the possibility of measuring the moment of inertia to even a 10% accuracy may provide stringent constraints on the nuclear equations of state [68–71]. The prospects for such a measurement improved significantly with the discovery of the binary pulsar PSR J0737-3039 [72, 73]. The first ever discovered double pulsar, PSR J0737-3039 exhibits characteristics that have enabled the accurate determination of several pulsar properties (such as the orbital period of the binary, both pulsar masses, and both spin periods) and have resulted in some of the most precise tests of Einstein's general theory of relativity.

Motivated by these facts, we have recently studied the sensitivity of the stellar moment of inertia to the equation of state [16]. However, we only found a mild sensitivity of the *total* moment of inertia to the underlying EOS. Thus, we redirected the main focus of such contribution to the *crustal* component of the moment of inertia. Several reasons prompted this choice. First, constraints on the EOS may be imposed from an analysis of pulsar glitches in the Vela pulsar that place at least a 1.4% of the total moment of inertia in the solid crust [59]. Second, the crust is thin and the density within it is low, so fairly accurate analytic expressions for the crustal moment of inertia have been developed in terms of two stellar properties that are highly sensitive to the EOS: (a) the radius of the uniform core and (b) the transition pressure at the core-crust interface [16, 59, 60]. Finally, given the strong correlation just found between the core-crust transition pressure P_t and $R_{\rm skin}$, one expects the emergence of a similar strong correlation between the crustal moment of inertia and $R_{\rm skin}$. Note, however, that our expectation of a strong correlation is solely based on the results of the covariance analysis. If instead one relies on a systematic variations around an optimal model, no strong correlation was found [16].

A	$\langle A\rangle \pm \Delta A$	$\rho(A, R_{\rm skin})$
$I^{\rm cr}_{0.8}$	(8.7777 ± 2.5612) [29.178%]	0.9781
$I^{\rm cr}_{1.4}$	(5.8988 ± 1.4055) [23.827%]	0.9619
$I_{0.8}$	(7.4067 ± 0.3204) [4.326%]	0.9299
$I_{1.4}$	(14.7660 ± 0.3437) [2.327%]	0.5192

TABLE V: Theoretical errors associated to the predictions of the FSUGold model for the crustal (in units of $10^{43}\,{\rm g\,cm^2}$) and total (in units of $10^{44}\,{\rm g\,cm^2}$) moment of inertia of a 0.8 and 1.4 solar-mass neutron star.

In Table V we list the crustal and total moment of inertia for neutron stars of 0.8 and 1.4 solar masses; the correlation coefficients are also displayed in graphical form in Fig. 7. As expected, the crustal moment of inertia—being sensitive to the core-crust transition pressure P_t—displays a strong correlation to $R_{\rm skin}$. Note that the large error attached to this observable reflects the large theoretical uncertainty associated with $R_{\rm skin}$—and ultimately with L. Given that the central density for a low-mass neutron star is only slightly larger than saturation density, the correlation between the total moment of inertia of a $0.8\,M_\odot$ neutron star and $R_{\rm skin}$ remains strong. However, we find a significant deterioration in the correlation between $R_{\rm skin}$ and the moment of inertia of a 1.4 solar-mass neutron star.

We close this section by collecting in Fig. 8 all correlation coefficients displayed earlier between $R_{\rm skin}$ and the large number of neutron-star observables. Moreover, we display in a color-coded format in Fig. 9 correlation coefficients for 16 observables (i.e., 120 independent pairs) of relevance to the structure, dynamics, and composition of neutron stars. As shown earlier, most of these stellar observables display a strong correlation—or anti-correlation—to the neutron skin thickness of ^{208}Pb (first column/row in Fig. 9). As mentioned above, a notable exception is the total moment of inertia of a canonical $1.4\,M_\odot$ neutron star. Of course, not every neutron-star observable is sensitive to the density dependence of the symmetry energy. The maximum neutron-star mass $M_{\rm max}$, with a correlation coefficient of

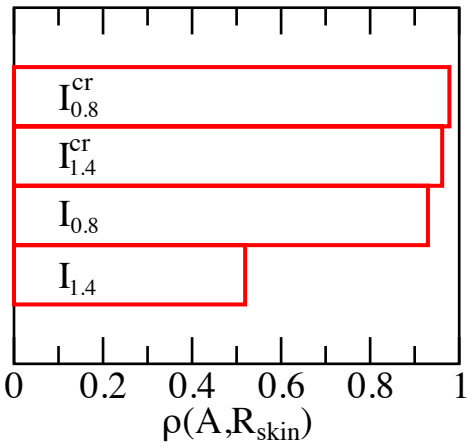

FIG. 7: (Color online) The correlation coefficient between the neutron-skin thickness of ^{208}Pb and various neutron-star properties of relevance to the crustal and total moment of inertia.

only $\rho(M_{\rm max}, R_{\rm skin}) = 0.0163$, provides a particularly clear example. Note, however, that $M_{\rm max}$ yields one of the best constraints—if not the best—on the high density component of the equation of state.

IV. CONCLUSIONS

The successfully commissioned Lead Radius Experiment (PREX) at the Jefferson Laboratory has provided the first largely model-independent determination of neutron-skin thickness of ^{208}Pb [12]: $R_{\rm skin} \equiv R_n - R_p = 0.33^{+0.16}_{-0.18}$ fm. Given that the determination of the neutron radius of a heavy nucleus is known to have strong implications on the structure, dynamics, and composition of neutron stars [2–4, 14–16, 74], a detailed covariance analysis was implemented to quantify the correlations between $R_{\rm skin}$ and a variety of neutron-star observables. Moreover, meaningful theoretical uncertainties were provided for all predicted observables. We note that although the significant impact of a measurement of $R_{\rm skin}$ on neutron-star properties has been known for almost a decade, our work quantifies for the first time these correlations on the basis of a detailed covariance analysis. We stress that the covariance analysis employed here represents the least biased and most comprehensive tool to uncover correlations between physical observables [7, 17].

In the present study we have computed correlation coefficients between $R_{\rm skin}$ and the following quantities of direct relevance to the physics of neutron stars: (a) the equation of state of pure neutron matter, (b) stellar radii, (c) the onset of the direct Urca proces, (d) the core-crust phase transition, and (e) the total and crustal moment of inertia. In addition to their intrinsic importance, these observables are interesting as they are sensitive to the density dependence of the symmetry energy over a wide range of densities. For example, whereas the onset of the direct Urca process is sensitive to the symmetry energy at high densities, the core-crust transition probes the symmetry energy at densities of about a third to a half of nuclear-matter saturation density.

Although most of the correlations follow the expected trend, two observables—both strongly correlated to $R_{\rm skin}$—deserve a special mention. These are the threshold proton fraction for the direct Urca process $Y_{\rm p}^{\rm Urca}$ and the core-crust transition pressure $P_{\rm t}$. First, the strong anti-correlation (of about -0.99) between $Y_{\rm p}^{\rm Urca}$ and $R_{\rm skin}$ came as a surprise because the sensitivity of $Y_{\rm p}^{\rm Urca}$ to the density dependence of the symmetry energy is due entirely to the presence of muons in the stellar core. Indeed, in the absence of muons $Y_{\rm p}^{\rm Urca}$ is fixed at 1/9 and the correlation coefficient vanishes. Second, the strong direct correlation between $P_{\rm t}$ and $R_{\rm skin}$ (of about $+0.95$) is surprising because no such correlation was observed in previous studies [16, 63, 65]. Note, however, that those earlier studies do not rely on a covariance analysis, but rather explore possible correlations by using either a large number of nuclear models [63, 65] or models that are systematically varied around an optimal one [16]. Although the covariance analysis implemented here provides the proper statistical measure of correlation between two observables [29], a covariance analysis can not assess *systematic* errors associated with the limitations of a given model. Thus, the implementation of a covariance analysis using other nuclear functionals is both highly desirable and strongly encouraged.

In connection to the follow-up PREX measurement that aims to achieve the original 1% precision goal, we regard it of a great value, as few accurately calibrated models—if any—predict such a large (central) value for $R_{\rm skin}$. Moreover, such a large neutron skin—which would imply a fairly stiff symmetry energy—will have widespread repercussions in the physics of neutron stars. It is worth mentioning, however, that a 10% uncertainty in the determination of the slope of the symmetry energy appears to require a more stringent measurement (at the 0.5% level) of the neutron radius of

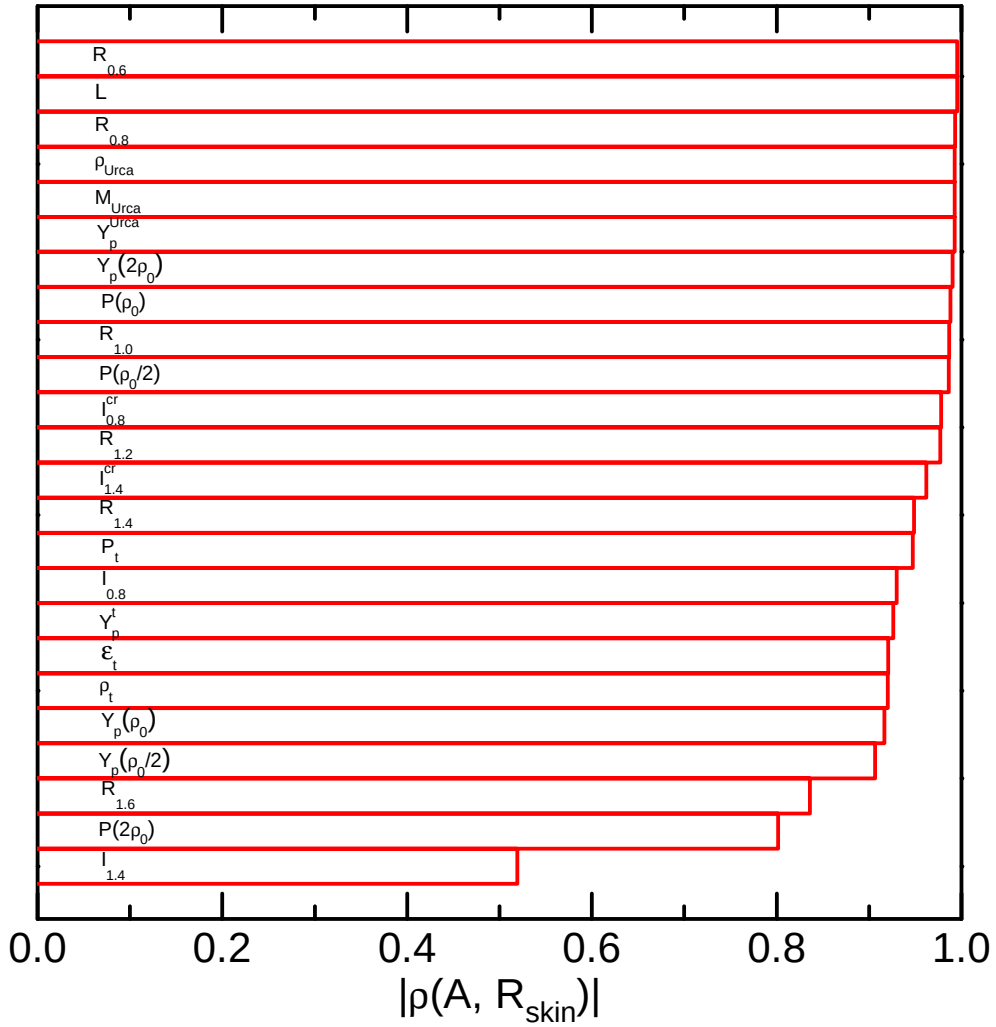

FIG. 8: (Color online) The correlation coefficient between the neutron-skin thickness of ^{208}Pb and the large number of neutron-star properties discussed in the text.

^{208}Pb [16, 75]. Ultimately, a determination of the density dependence of the symmetry energy is likely to require a multi-pronged approach [26]. First, from the theoretical perspective, we expect that powerful arguments based on the universality of dilute Fermi gases in the unitary regime will continue to shed valuable insights into the behavior of pure neutron matter. Second, in terms of laboratory observables, the dipole polarizability of ^{208}Pb—measured recently with unprecedented accuracy [76]—provides a unique constraint on the density dependence of the symmetry energy and an excellent complement to the neutron-skin thickness of ^{208}Pb [13]. Finally, enormous advances in both land- and spaced-based observatories have started to impose significant constraints on the equation of state. In this work we have demonstrated the existence of many neutron-star observables that—by virtue of their strong correlation—may be used as a proxy for $R_{\rm skin}$. A particularly interesting alternative is the radius of a low-mass neutron star, as its central density is close to nuclear-matter saturation density. Indeed, the radius of $0.8\,M_\odot$ neutron star, $R_{0.8}$, displays a strong correlation (of $\sim$0.99) to $R_{\rm skin}$. Thus, a 5% measurement of $R_{0.8}$ would translate into a $\sim$0.4% constraint on the neutron radius of ^{208}Pb. Unfortunately, the measurement of stellar radii remains a serious challenge that is further complicated by the scarcity of low-mass neutron stars. Given that most well measured neutron-star masses lie within a narrow range centered around $1.4\,M_\odot$, low-mass neutron stars may be difficult to form and therefore may not even exist. In such a case, a highly accurate measurement of $R_{\rm skin}$ remains the sole alternative.

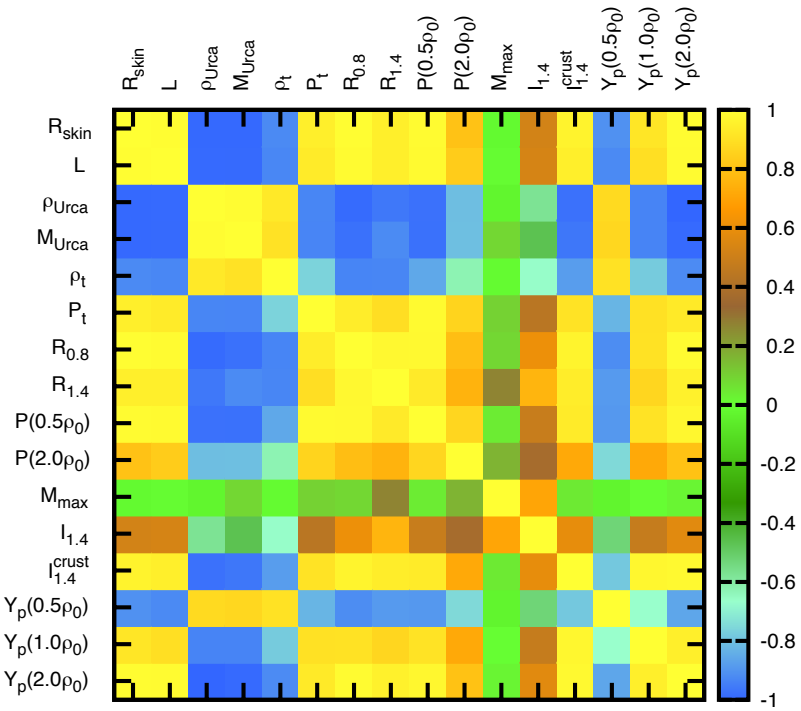

FIG. 9: (Color online) Color-coded plot of the 120 independent correlation coefficients between 16 physical observables of relevance to the structure and dynamics of neutron stars.

Acknowledgments

This work was supported in part by the United States Department of Energy under grant DE-FG05-92ER40750 (FSU), by the National Aeronautics and Space Administration under grant NNX11AC41G issued through the Science Mission Directorate, and by the NSF grant PHY-1068022 (TAMUC). We would like to dedicate this work to the memory of our dear friend and colleague Professor Brian D. Serot.

[1] R. J. Furnstahl, Nucl. Phys. **A706**, 85 (2002).
[2] C. J. Horowitz and J. Piekarewicz, Phys. Rev. **C64**, 062802 (2001).
[3] C. J. Horowitz and J. Piekarewicz, Phys. Rev. Lett. **86**, 5647 (2001).
[4] A. W. Steiner, M. Prakash, J. M. Lattimer, and P. J. Ellis, Phys. Rept. **411**, 325 (2005).
[5] B.-A. Li, L.-W. Chen, and C. M. Ko, Phys. Rept. **464**, 113 (2008).
[6] The Editors, Phys. Rev. A **83**, 040001 (2011).
[7] F. J. Fattoyev and J. Piekarewicz, Phys. Rev. **C84**, 064302 (2011).
[8] B. A. Brown, Phys. Rev. Lett. **85**, 5296 (2000).
[9] M. Centelles, X. Roca-Maza, X. Vinas, and M. Warda, Phys. Rev. Lett. **102**, 122502 (2009).
[10] M. Centelles, X. Roca-Maza, X. Vinas, and M. Warda, Phys. Rev. **C82**, 054314 (2010).
[11] I. Vidana, C. Providencia, A. Polls, and A. Rios, Phys. Rev. **C80**, 045806 (2009).
[12] S. Abrahamyan *et al.*, Phys. Rev. Lett. **108**, 112502 (2012).
[13] J. Piekarewicz *et al.*, arXiv:1201.3807 (2012).
[14] J. Carriere, C. J. Horowitz, and J. Piekarewicz, Astrophys. J. **593**, 463 (2003).
[15] C. J. Horowitz and J. Piekarewicz, Phys. Rev. **C66**, 055803 (2002).
[16] F. J. Fattoyev and J. Piekarewicz, Phys. Rev. **C82**, 025810 (2010).
[17] P.-G. Reinhard and W. Nazarewicz, Phys. Rev. **C81**, 051303 (2010).
[18] B. G. Todd-Rutel and J. Piekarewicz, Phys. Rev. Lett **95**, 122501 (2005).
[19] J. D. Walecka, Annals Phys. **83**, 491 (1974).
[20] B. D. Serot and J. D. Walecka, Adv. Nucl. Phys. **16**, 1 (1986).
[21] D. H. Youngblood, H. L. Clark, and Y.-W. Lui, Phys. Rev. Lett. **82**, 691 (1999).
[22] J. Piekarewicz, Phys. Rev. **C64**, 024307 (2001).

[23] J. Piekarewicz, Phys. Rev. **C66**, 034305 (2002).
[24] G. Colò, N. Van Giai, J. Meyer, K. Bennaceur, and P. Bonche, Phys. Rev. **C70**, 024307 (2004).
[25] H. Mueller and B. D. Serot, Nucl. Phys. **A606**, 508 (1996).
[26] J. Piekarewicz, Phys. Rev. **C76**, 064310 (2007).
[27] P. Demorest, T. Pennucci, S. Ransom, M. Roberts, and J. Hessels, Nature **467**, 1081 (2010).
[28] F. J. Fattoyev, C. J. Horowitz, J. Piekarewicz, and G. Shen, Phys. Rev. **C82**, 055803 (2010).
[29] S. Brandt, *Data Analysis: Statistical and Computational Methods for Scientists and Engineers* (Springer, New York, 1999), 3rd ed.
[30] A. Schwenk and C. J. Pethick, Phys. Rev. Lett. **95**, 160401 (2005).
[31] A. Gezerlis and J. Carlson, Phys. Rev. **C81**, 025803 (2010).
[32] A. Gezerlis and J. Carlson, arXiv:1109.4946 (2011).
[33] S. Gandolfi, A. Y. Illarionov, K. Schmidt, F. Pederiva, and S. Fantoni, Phys. Rev. **C79**, 054005 (2009).
[34] L. Lindblom, Astrophys. J. **398**, 569 (1992).
[35] S. Thorsett and D. Chakrabarty, Astrophys. J. **512**, 288 (1999).
[36] F. Ozel, G. Baym, and T. Guver, Phys. Rev. **D82**, 101301 (2010).
[37] A. W. Steiner, J. M. Lattimer, and E. F. Brown, Astrophys. J. **722**, 33 (2010).
[38] V. Suleimanov, A. Y. Potekhin, and K. Werner, Adv. Space Res. **45**, 92 (2010).
[39] F. J. Fattoyev and J. Piekarewicz, Phys. Rev. **C82**, 025805 (2010).
[40] V. Suleimanov, J. Poutanen, M. Revnivtsev, and K. Werner, Astrophys. J. **742**, 122 (2011).
[41] J. M. Lattimer, C. J. Pethick, M. Prakash, and P. Haensel, Phys. Rev. Lett. **66**, 2701 (1991).
[42] C. Pethick, Rev. Mod. Phys. **64**, 1133 (1992).
[43] J. M. Lattimer and M. Prakash, Science **304**, 536 (2004).
[44] D. Page, J. M. Lattimer, M. Prakash, and A. W. Steiner, Astrophys. J. Suppl. **155**, 623 (2004).
[45] R. Cavagnoli, D. P. Menezes, and C. Providencia, Phys. Rev. **C84**, 065810 (2011).
[46] S. Weissenborn, D. Chatterjee, and J. Schaffner-Bielich (2011), 1112.0234.
[47] G. Baym, C. Pethick, and P. Sutherland, Astrophys. J. **170**, 299 (1971).
[48] D. G. Ravenhall, C. J. Pethick, and J. R. Wilson, Phys. Rev. Lett. **50**, 2066 (1983).
[49] M. Hashimoto, H. Seki, and M. Yamada, Prog. Theor. Phys. **71**, 320 (1984).
[50] C. P. Lorenz, D. G. Ravenhall, and C. J. Pethick, Phys. Rev. Lett. **70**, 379 (1993).
[51] G. Watanabe, K. Sato, K. Yasuoka, and T. Ebisuzaki, Phys. Rev. **C68**, 035806 (2003).
[52] G. Watanabe, T. Maruyama, K. Sato, K. Yasuoka, and T. Ebisuzaki, Phys. Rev. Lett. **94**, 031101 (2005).
[53] C. J. Horowitz, M. A. Perez-Garcia, and J. Piekarewicz, Phys. Rev. **C69**, 045804 (2004).
[54] T. Maruyama, T. Tatsumi, D. N. Voskresensky, T. Tanigawa, and S. Chiba, Phys. Rev. **C72**, 015802 (2005).
[55] A. W. Steiner, Phys. Rev. **C77**, 035805 (2008).
[56] S. Avancini *et al.*, Phys. Rev. **C78**, 015802 (2008).
[57] W. G. Newton and J. R. Stone, Phys. Rev. **C79**, 055801 (2009).
[58] J. Xu, L.-W. Chen, B.-A. Li, and H.-R. Ma, Astrophys. J. **697**, 1549 (2009).
[59] B. Link, R. I. Epstein, and J. M. Lattimer, Phys. Rev. Lett. **83**, 3362 (1999).
[60] J. M. Lattimer and M. Prakash, Astrophys. J. **550**, 426 (2001).
[61] A. W. Steiner and A. L. Watts, Phys. Rev. Lett. **103**, 181101 (2009).
[62] C. J. Horowitz and K. Kadau, Phys. Rev. Lett. **102**, 191102 (2009).
[63] C. Ducoin, J. Margueron, and C. Providencia, Europhys. Lett. **91**, 32001 (2010).
[64] S. S. Avancini, S. Chiacchiera, D. P. Menezes, and C. Providencia, Phys. Rev. **C82**, 055807 (2010).
[65] C. Ducoin, J. Margueron, C. Providencia, and I. Vidana, Phys. Rev. **C83**, 045810 (2011).
[66] J. B. Hartle, Astrophys. J. **150**, 1005 (1967).
[67] J. B. Hartle and K. S. Thorne, Astrophys. J. **153**, 807 (1968).
[68] I. A. Morrison, T. W. Baumgarte, S. L. Shapiro, and V. R. Pandharipande, Astrophys. J. **617**, L135 (2004).
[69] J. M. Lattimer and B. F. Schutz, Astrophys. J. **629**, 979 (2005).
[70] M. Bejger, T. Bulik, and P. Haensel, Mon. Not. Roy. Astron. Soc. **364**, 635 (2005).
[71] G. Lavagetto, I. Bombaci, A. D'Ai', I. Vidana, and N. R. Robba (2006).
[72] M. Burgay *et al.*, Nature. **426**, 531 (2003).
[73] A. G. Lyne *et al.*, Science **303**, 1153 (2004).
[74] B.-A. Li and A. W. Steiner, Phys. Lett. **B642**, 436 (2006).
[75] X. Roca-Maza, M. Centelles, X. Vinas, and M. Warda, Phys. Rev. Lett. **106**, 252501 (2011).
[76] A. Tamii *et al.*, Phys. Rev. Lett. **107**, 062502 (2011).